Assessment of transient EMI impact on LTE communications using EVM & PAPR

Olivier Stienne, Virginie Deniau, Eric Pierre Simon

▶ **To cite this version:**

Olivier Stienne, Virginie Deniau, Eric Pierre Simon. Assessment of transient EMI impact on LTE communications using EVM & PAPR. IEEE Access, 2020, 8, pp.227304-227312. 10.1109/access.2020.3045666 . hal-03127227

HAL Id: hal-03127227
https://hal.science/hal-03127227

Submitted on 1 Feb 2021

HAL is a multi-disciplinary open access archive for the deposit and dissemination of scientific research documents, whether they are published or not. The documents may come from teaching and research institutions in France or abroad, or from public or private research centers.

L'archive ouverte pluridisciplinaire **HAL**, est destinée au dépôt et à la diffusion de documents scientifiques de niveau recherche, publiés ou non, émanant des établissements d'enseignement et de recherche français ou étrangers, des laboratoires publics ou privés.

Distributed under a Creative Commons Attribution 4.0 International License

IEEE Access
Multidisciplinary | Rapid Review | Open Access Journal

Received November 18, 2020, accepted December 6, 2020, date of publication December 17, 2020,
date of current version December 31, 2020.

Digital Object Identifier 10.1109/ACCESS.2020.3045666

Assessment of Transient EMI Impact on LTE Communications Using EVM & PAPR

OLIVIER STIENNE[1], VIRGINIE DENIAU[2], AND ERIC PIERRE SIMON[3]
[1]Icam, 59800 Lille, France
[2]COSYS, Gustave Eiffel University, Lille Campus, 59650 Villeneuve d'Ascq, France
[3]IEMN-Telice, Lille University, F-59655 Villeneuve d'Ascq, France

Corresponding author: Olivier Stienne (olivier.stienne@icam.fr)

This work was performed in the framework of the ELSAT2020 project, which is co-financed by the European Union with the European Regional Development Fund, the French state and the Hauts de France Region Council.

ABSTRACT The brief contact losses between the pantograph and the catenary in high-speed trains create transient interferences, which extend to the frequency bands used by telecommunication systems. This article presents a study of the impact of these transient wideband interferences on LTE communications between the train and a base station. In this study, we set up an experimental test bench, which establishes LTE communication between a communication tester and a USB/LTE dongle in the presence of transient interferences. We analysed the impact of these interferences on the error vector magnitude (EVM) of the received LTE signals and we observed that the EVM evolution does not explain certain communication interruptions. Indeed, interruptions can occur for EVM values significantly inferior to the standard limits. To understand the relationship between the interference characteristics and the communication interruption, we studied the peak to average power ratio (PAPR). Indeed, the PAPR is well suited to analyse transient interferences because it evolves with the amplitude but also with the repetition of the transient. Then, the PAPR measurement can provide a diagnostic assistance to analyse whether along certain railway lines, pantograph-catenary interferences are the cause of the LTE interruptions.

INDEX TERMS Electromagnetic interferences and disturbances (EMI), transient interferences, long terme evolution (LTE), LTE quality indicators, error vector magnitude (EVM), peak to average power ratio (PAPR), interference to signal ratio (ISR).

I. INTRODUCTION

Currently, LTE technology provides new services to users such as Internet access via a WiFi-LTE gateway on high-speed trains. The railway companies have agreements with mobile operators so that LTE train ground connections are sized for passengers needs on board trains [1]–[3]. LTE is also being considered for future railway uses, such as automated train systems or autonomous trains [4], [5]. Indeed, 4G also called LTE is being considered for remote train control applications, as presented at the 12th World Congress on Railway Research, 2019 [6]. In this system, the LTE communication would be used to transmit the video from the track to the driver cab located on the ground side and to transmit the train control information. In such critical applications, it is essential that the LTE communications be reliable.

The associate editor coordinating the review of this manuscript and approving it for publication was Xiaofei Wang.

However, the railway environment is rich in electromagnetic interferences (EMI). One of the disturbance main sources is due to the electric sparks created by the catenary-pantograph sliding contact. This generates electromagnetic emissions, which range from a few dozen Hz to a few GHz [7]. These transient electromagnetic interferences can disturb the reception of the antennas mounted on train roofs and provoke the loss of radio communications as shown in Figure 1.

Few studies speak of the constraints linked to fast transient interferences for on-board LTE communications. Recently, a study of the disturbances due to the catenary-pantograph arc on the quality of an LTE-R TDD (Time-Division Duplex) signal in the 400 MHz band has been carried out [8].

Here, we examine the behavior of LTE-FDD communication in the 900MHz band face to transient interferences.

In fact, LTE supports, on the radio level, time multiplexing, TDD (Time-Division Duplex), used in China and frequency multiplexing, FDD (Frequency Division Duplexing), used in

This work is licensed under a Creative Commons Attribution 4.0 License. For more information, see https://creativecommons.org/licenses/by/4.0/

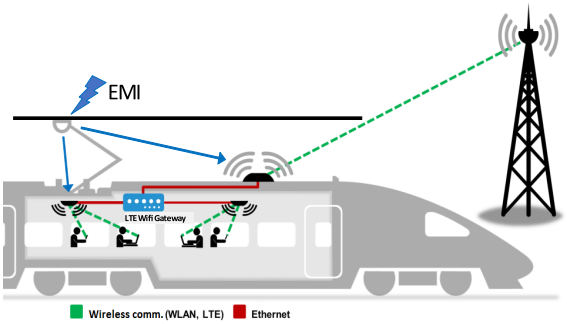

FIGURE 1. Sliding contacts disturbances in the railway environment.

Europe. LTE-TDD and LTE-FDD are presented and compared in articles [9], [10].

In FDD, two distinct frequency bands are used, one for transmitting from the base station to the user equipment (downlink) and the other for transmitting from the user equipment to the base station (Uplink). Moreover, while [8] was based on simulations, we adopt an experimental approach to take into account all the components of a reception chain, and thus bring up issues that do not appear in the simulation. Our work studies the LTE communication behavior in the face of fast transient interferences in the following way: first, LTE communication is established between a radio-communication tester and a USB/LTE dongle. Second, a test bench introduces transient interferences at the uplink level of LTE communication. Finally, the quality of LTE signals is measured by the radio-communication tester and the interferences and communication signals characteristics are simultaneously measured by the oscilloscope. Unlike other studies which use the BER (bit error rate) [8], [11], in our work, the EVM is used to measure the LTE signal quality. The reason is that the BER is not available at the receiver, only the BLER (block error rate) is. However, to determine the BLER, it is necessary to demodulate the signal received and to count the acknowledgment and non-acknowledgement (ACK and NACK). Then, the BLER assesses the performance of the communication system but it involves upper layers and it is difficult to link the variation of the BLER with the occurrence of specific interferences. It is better to stick to the physical layer to assess such interferences, by using the EVM. EVM is widely applied as a signal quality conformity measure of digital transmitters/receivers in modern communication systems [8], [12], [13].

EVM is the difference between the expected value of a symbol represented by a demodulated complex voltage and the value of the symbol actually received. In this article, electromagnetic interferences are added to the uplink transmission signal. These transient interferences are characterized by their amplitude and their repetition time. The impact of these two parameters on the LTE communication quality is studied by varying the amplitude for different transient interference repetition periods.

Our measurement results allow us to understand how these rapid transient interferences can degrade communication quality, or even interrupt the LTE communication.

During the tests, we were able to observe communication breakdowns for EVMs well below the standard limit thresholds. The EVM cannot alone therefore indicate the effect of transient interferences on LTE communication.

In view of the measurement problems observed during the experiments, the PAPR was introduced as an indicator [14], [15]. PAPR is not usually used as a quality indicator of the received signal, but it seems relevant for analyzing the LTE communication reliability in the face of fast transient interferences. It makes it possible to observe direct links between transient interferences and communication cutoff.

These communication breakdowns can appear during journeys in high-speed trains. The study thus introduces an indicator allowing to know whether these transient interferences are the reason of the communication interruptions. This therefore constitutes a diagnostic aid in order to design more robust LTE communication in the rail environment. Another positive aspect of using the PAPR is that the monitoring of this indicator can be carried out by an external system independently from the communication equipment, such as an oscilloscope. It does not require implementing the first stages of the LTE communication system.

To sum up, the contributions of this article are as follows:

- Selection of an indicator, the PAPR, indicative of the presence of transient interferences.
- Contribution to a new diagnostic tool to analyze the impact of transient interferences on LTE communication, based on the PAPR.
- In case of LTE communication breakdown, the diagnostic tool is able to state if the transient interference is the cause or not.
- Implementation of the diagnostic tool external to the communication terminals.
- Results based on experiments that consider all the components, including the RF chain, of LTE systems currently deployed.

After the introduction, in section 2, the article presents the model used to achieve the rapid transient interferences. Section 3 is dedicated to the test bench and its functions. Section 4 presents the EVM (error vector magnitude) as an indicator of the LTE communication quality at the physical layer level. Finally, section 5 focuses on the CF (crest factor) or rather the PAPR (Peak to Average Power Ratio) which characterizes an RF signal. In conclusion, the measurement results are analysed.

II. THE TRANSIENT INTERFERENCE MODEL

The catenary-pantograph contact generates transient broadband electromagnetic phenomena. There are many studies on the characterization of fast radiated transient disturbances due to sliding contacts of the pantograph on the catenary

under a spectral approach as in article [16], under a temporal approach as in article [17] or both as in articles [18], [19].

The resulting model depends on the acquisition method (position of the antenna relative to the electric arc, type of antenna, frequency band studied, bandwidth of the antenna, the measurement sampling…) as described in articles [20], [21].

In the RailCom project [17], [22], [23], acquisition campaigns were carried out on high-speed trains to measure the emissions received by the GSM-R antenna due to catenary-pantograph contact losses. Measurements of the signal received by the train GSM-R antenna were taken using an oscilloscope at a 10Gsps sampling frequency, in the 900MHz frequency band. They were analyzed in order to define the characteristics of the transient interference and to define a model usable in the laboratory. The model $s_{trans}(t)$ obtained is a signal modulated on the central frequency f_c of the RF band that must be disturbed. The envelope shape of the signal $s_{trans}(t)$ is given by an exponential double function whose parameters are t_{rise} and t_{hold}. t_{rise} is the rise time between 10% and 90% of the signal and t_{hold} is the hold time at 50% of the peak signal. The signal $s_{trans}(t)$ is represented by the following equation:

$$s_{trans}(t) = A_0 \cdot \left(e^{\frac{-t}{t_{rise}}} - e^{\frac{-t}{t_{hold}}} \right) \cdot \sin(2\pi f_C t) \cdot u(t) \qquad (1)$$

where, A_0 is the signal amplitude, and $u(t)$ is the step unit function.

By modulating the signal on the studied RF frequency, the effect of the fast transient signal is limited to the studied bandwidth. The parameters of the model noted for the statistical studies carried out on fast transient interferences [16], [17] give rise times and hold times in the following ranges:

- t_{rise}, the rise time is between 0.1ns and 3ns
- t_{hold}, the hold time is between 1ns and 50ns

The modeling made it possible to study the behavior of a GSM-R communication in the face of transient disturbances in the laboratory.

However, these studies were carried out for a GSM-R communication system. To keep this model valid, we conducted our study in the LTE band 8, 900MHz (Table 5.2-1 and Table 5.6-1 of the E-UTRA frequency bands in 3GPP TS36.101 version 8) [24], which covers the same frequency bands as the GSM-R [25], [26].

For LTE communications, the parameters of the model (1) are chosen to disturb the uplink subcarriers equally (Δf=15kHz), and without disturbing the downlink band.

For the model, the carrier frequency is the center frequency of the uplink in band 8, i.e. here the frequency of 897.5MHz. The possible bandwidths, BW, in band 8 are 1.4MHz, 3MHz, 5MHz and 10MHz. By taking a rise time of 2ns and a hold time of 20ns, which gives us the temporal representation of Figure 2a with a variation less than 2dB on the LTE uplink band Figure 2b. Furthermore, these interferences do not disturb the downlink signal as shown by the spectral representation Figure 2b.

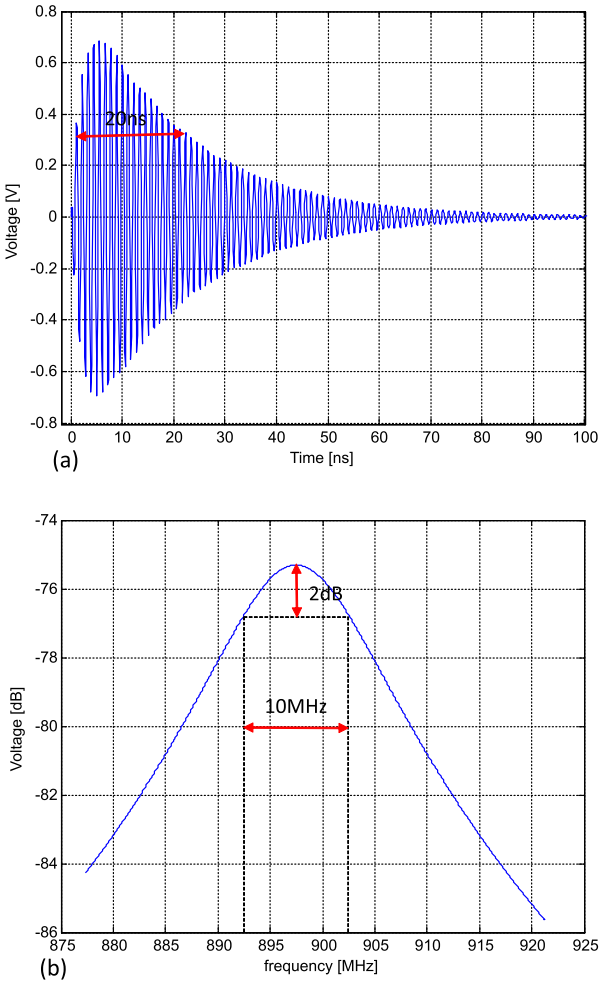

FIGURE 2. 2/20ns transient interference spectral and temporal representations.

The repetition time between two consecutive arcs is mainly due to the mechanical factors of the catenary-pantograph connection and the speed of the train. According to the results of the measurements in the study [17], these transient disturbances appear with repetition times that can vary from a few microseconds to several hundred microseconds. The impact of this repetition time on LTE communication is studied in Sections IV-B and V. For our study, the parameters of the model must remain consistent with the statistical studies carried out on fast transient disturbances [16], [17].

This model is added to LTE communication to disturb the uplink, using an arbitrary signal generator. The test bench presented in Figure 3 is used to establish LTE communication, to configure the interference, to view and record the measurements.

III. LTE TEST BENCH

The test bench allows us to study the impact of fast transient interferences on LTE communications as a function of the amplitude and for different values of the transient interference repetition period. In order to ensure the reproducibility and repeatability of the measurements, a conducted test bench has

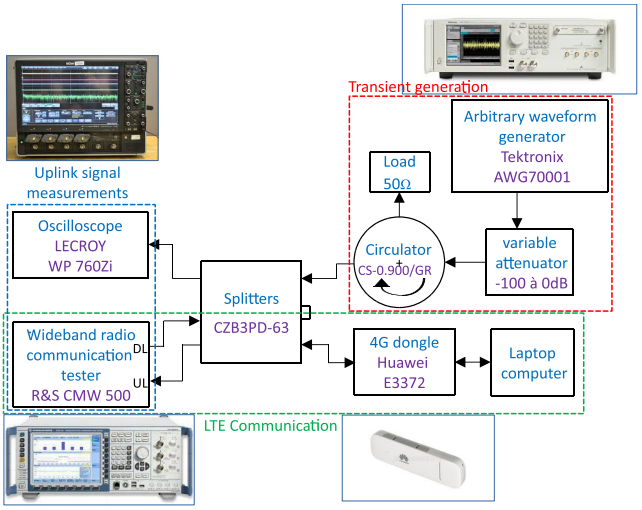

FIGURE 3. Test bench for LTE communications and transient interferences.

been implemented. That means that instead of using antennas, the input and output of the devices are connected with cables. This avoids radiating transient interferences and LTE communications in the test environment which can affect the public wireless communications. Moreover, the conducted mode also prevents the experiment results from being impacted by external disturbances.

The test bench presented in Figure 3 consists of 3 parts:

- LTE communication,
- transient interference generator,
- signals measurement.

Splitters connect the test bench different parts.

A. LTE COMMUNICATION

This LTE network emulation is carried out by a radio-communication tester, the CMW500 from R&S for the evolved node B (eNodeB) and the evolved packet core (EPC) of the LTE network [11]. This equipment allows us to emulate a real eNodeB with all layers of the LTE with access to many quality indicators. This type of device is used by manufacturers to test their terminals in real-world conditions before marketing their products. The RF chain is therefore composed of devices (band filter, duplexer, LNA, channel filter) fully compliant with the LTE materials currently deployed. A USB/LTE dongle, E3372 from Huawei compatible with band 8 is used as a user equipment (UE). It is connected to the splitter using an external shielded cable to transmit the LTE downlink and uplink communication signals. The radio-communication tester configures the LTE communication parameters such as the transmission power of the downlink defined by the RS-EPRE (Reference Signal-Energy per Resource Element) here at −50dBm/15kHz and the transmission power of the uplink transmitted by physical channels (PUSCH/PUCCH) from the UE to eNodeB, the LTE band used (here band 8), the modulation scheme (QPSK) and the bandwidth BW (1.4MHz, 3MHz, 5MHz and 10MHz).

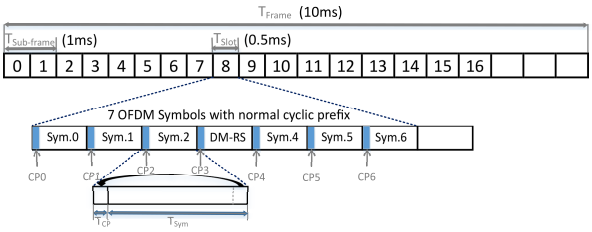

FIGURE 4. LTE Radio Frame structure.

B. TRANSIENT INTERFERENCES GENERATOR

An arbitrary waveform generator, the AWG 70001, is used to create rapid transient interferences from models defined previously with Matlab. A variable attenuator connected to the output of the arbitrary waveform generator varies the transient interference amplitude, which is added to the LTE uplink communication signal. A circulator isolates the generator from other communication signals.

C. SIGNALS MEASUREMENT

The radio-communication tester CMW500, can perform a large number of tests on the physical and MAC layers of LTE communication. These tests are defined in the 3GPP specification TS36.521 [27] to determine the UE conformity to LTE communication. For our measurements, we used the E-UTRA test model (E-TM) defined by 3GPP TS36.521-1. The test models (E-TM) are a set of signals for standard testing of the LTE device transmitter chain in SISO and for a single user. The implementation of these tests with the CMW500 is described in the application note from R&S [28].

An oscilloscope allows us to visualize the received RF signal. It is placed in the same measurement plane as the CMW500 input.

In Equation (2), the measurement noise and the propagation channel for the received signal are neglected, the received signal $s_{rx}(t)$ is only the addition of the uplink LTE communication signal $s_{LTE}(t)$ and fast transient interferences $\alpha \cdot s_{trans}(t)$ and α varies the transient interferences amplitude.

$$s_{rx}(t) = \alpha \cdot s_{trans}(t) + s_{LTE}(t) \tag{2}$$

Oscilloscope measurements are carried out with a 10Gsps sampling frequency and for a 1ms duration, corresponding to LTE subframe $T_{Sub-frame}$.

In Figure 4, we can see the subframe made up of 2 slots, the time of a slot T_{Slot} is 0.5ms. A slot contains 7 symbols of 66.67μs duration T_{Sym} with their cyclic prefixes with a 5.21μs duration T_{CP} for the first and 4.69μs the six others as we can see in Table 1.

IV. EVM MEASUREMENT

A. EVM MEASUREMENT METHOD

To detect problems in the communication environment or to assess the quality of LTE communications, the EVM measurement is generally considered sufficient [12], [13]. The evolution of EVM can be observed as a function of the interference to the LTE signal power ratio (ISR). The ISR (3)

TABLE 1. Table of LTE Parameters

Channel bandwidth	1.4MHz	3MHz	5MHz	10MHz
Resource Blocks	6	15	25	50
Symbol lenght	$66.67\mu s$			
Cyclic prefix length for symbol 0	$5.21\mu s$			
Cyclic prefix length for symbols 1 to 6	$4.69\mu s$			
EVM window length W samples	5	12	32	66

TABLE 2. Maximum Requirements for EVM

Parameter	Average EVM Level
QPSK or BPSK	17.5%
16QAM	12.5%
64QAM	to be defined

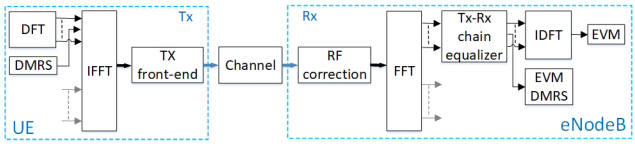

FIGURE 5. EVM measurement method according to TS36.101 release 8.

is calculated from the RMS voltages of sampled signals. The signals are measured with an oscilloscope, during a subframe of 1ms. ISR value is given by:

$$ISR = \sqrt{\frac{\frac{1}{N}\sum_{n=1}^{N}(\alpha \cdot s_{trans}(nT_s))^2}{\frac{1}{N}\sum_{n=1}^{N}(s_{LTE}(nT_s))^2}} \quad (3)$$

where, T_s is the oscilloscope sampling period, N is the number of samples at 10Gsps for 1ms, α is the value of the variable attenuator, $s_{trans}(nT_s)$ is the measurement value of the generator transient signal, $s_{LTE}(nT_s)$ is the measurement value of the uplink signal from the USB/LTE dongle.

For the EVM measurement, we rely on two specifications: 3GPP TS36.101 [24] on UE radio transmission, reception and 3GPP TS36.521 [27] on UE conformity specifications in transmission reception. The 3GPP specification TS36.101 [24] defines the signal quality requirements in the channel. EVM is one of these requirements and is presented in paragraph 6.5 of the specification in its version 8. Table 2 defines the EVM limit values not to be exceeded for a correct LTE connection.

[24] also defines the EVM measurement in the reception chain of the LTE signal. The EVM values by symbol are obtained after RF correction, switching to baseband, FFT, equalization and IDFT (Inverse Discrete Fourier Transform). But the EVM value of the reference symbol, the DM-RS (DeModulated Reference Signal), is obtained directly after equalization without IDFT as shown in Figure 5.

The 3GPP specification TS36.521 [27] gives the measurement procedures for LTE terminals and presents transmission

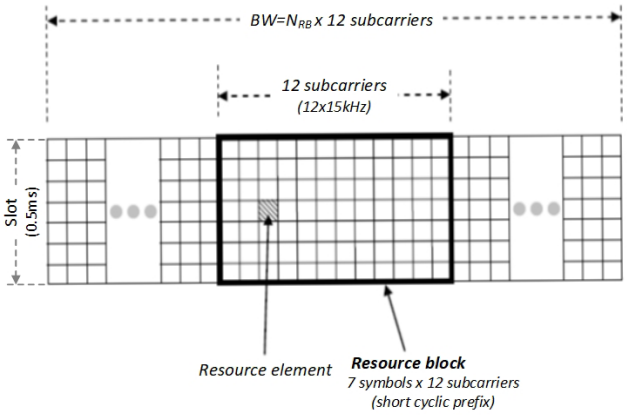

FIGURE 6. LTE radio grid structure.

characteristics, reception characteristics and performance requirements in LTE communication context.

[27] describes the measurement conditions and the measurements to be performed for an LTE transmission in accordance with this test specification. The test bench around the radio-communication tester and the EVM measurements are therefore carried out according to the 3GPP specification TS36.521-1 and using the application note R&S [28]. The EVM calculation method is detailed in appendix E of the 3GPP specification TS36.521 [27].

The EVM is the quadratic mean of the subtraction between the ideal signal and the real signal, received for a QPSK or 16-QAM modulation scheme, contained in an element resource on allocated resource blocks. Figure 6 presents the resource block constitution with its 12 subcarriers spaced by 15 kHz, over a 0.5 ms slot. The slot contains 7 symbols, including a reference symbol (DM-RS). The quadratic average on the subcarriers of this resource block gives the EVM value per symbol. For LTE, the final EVM value is the higher between two EVM measured averages at two different moments, called EVM_{low} and EVM_{high}. The low and high positions correspond to the start of the FFT calculation window for a symbol duration. These low and high positions are placed at the beginning and at the end of the cyclic prefix. The interval between the low and high locations is defined by the parameter W in Table 1. In the LTE communications, the channel bandwidth, the modulation type and the power levels are parameters that can vary over time depending on the quality of the services required and the transmission conditions (coverage, interference, channel model). However, in this preliminary study, it was essential to be able to interpret and verify the repeatability of the results. Therefore, we imposed fixed values for these different parameters: band 8, QPSK modulation, central frequencies of 897.5MHz for the uplink and 942.5MHz for the downlink and channel bandwidth of 1.4MHz, 3MHZ, 5MHz and 10MHz. The power levels of the uplink and downlink were set in accordance with TS36.521-1 recommendations for "E-TM" testing modes for LTE communications [27], [28].

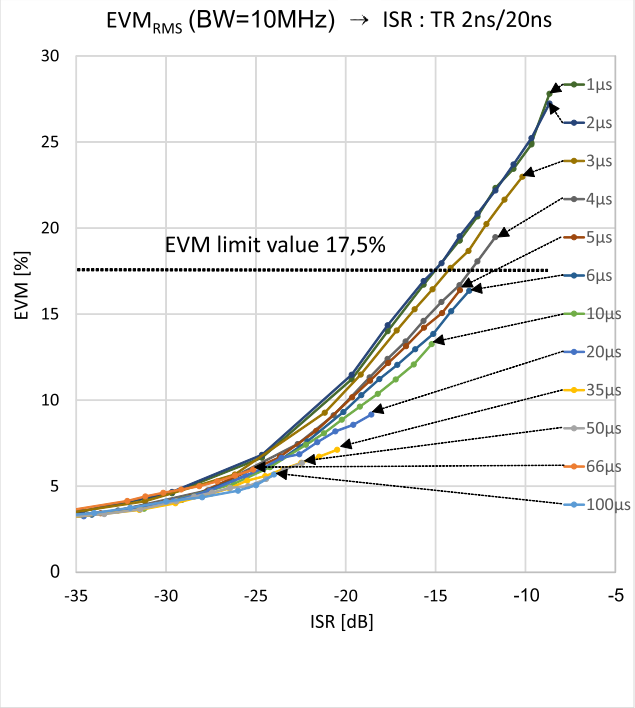

FIGURE 7. EVM function of the ISR for a 10MHz BW.

B. EVM MEASUREMENT IN THE PRESENCE OF INTERFERENCES

In order to study the impact of the transient interference repetition time, the interference signal is repeatively generated with fixed interval times, ranging from 1μs to 100μs. These repetition interval times have been set according to the representative time values of LTE signal such as the symbol duration or the cyclic prefixes duration, presented in Table 1. Indeed, the 1μs minimum repetition time is less than the 4.69μs cyclic prefix duration T_{CP} and the 100μs maximum repetition time is greater than the 66.67μs symbol duration T_{Sym}.

For the different transient interference repetition times, the obtained EVM is presented as a function of the ISR Figure 7 for a bandwidth of 10MHz. When the LTE communication is established, the transient interference amplitude value is gradually increased using the variable attenuator represented by α in the Equation (3) until the communication is cut off. The maximum admissible EVM value, 17.5%, for a QPSK modulation scheme, is given in Table 2. In Figure 7 when the ISR increases, the communication can be cut off for EVM values well inferior to the 17.5% limit. For a 100μs interval time, the EVM value at the communication cutoff is 5.7%. On the other hand, for a 1μs interval repetition time, the EVM value at the communication cutoff reaches 27.8%, which is higher than the limit value given in Table 2. Then, when the time interval between transient interference increases, the EVM value at the communication cutoff decreases. In addition to the results in Figure 7 for a 10MHz bandwidth, EVM measurements were also carried out for the BW of 1.4MHz, 3MHz and 5MHz and the results presented similar trends.

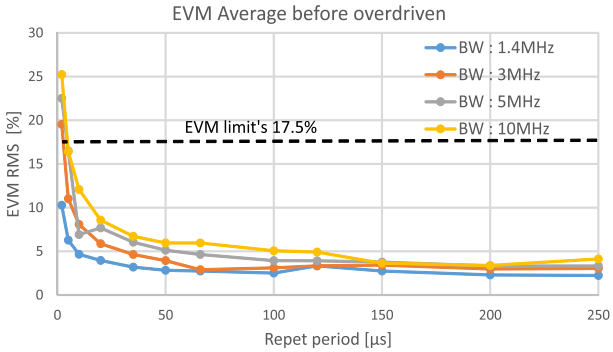

FIGURE 8. EVM value as a function of the transient repetition interval time at the loss of communication.

Figure 8 focuses on the EVM values at the communication cutoff moment according to the interference repetition times which go from 1μs to 250μs and for different LTE communication BW.

In most cases, communication is lost without reaching the EVM limit value. When the repetition times are lower than 120μs, the larger the BW is and more the EVM seems sensitive to transient interferences. For repetition interval times inferior to 5μs, the EVM value before cutoff depends on the LTE communication BW; the larger the BW, the higher the EVM limit value. For repetition interval times greater than 5μs, whatever the BW used, the LTE communication is cut by transient interferences without reaching the 17.5% EVM limit value. For interference repetition times greater than 100μs, communication is cut off for EVM less than 5%.

While analysing the causes of communication losses, we noticed in the radio-communication tester report, an error message mentioning the crest factor excess at the reception of the LTE uplink signal.

V. HARMONIC DISTORTION INDICATOR: CF, PAPR

The crest factor is useful for drawing attention to the presence of undesired high peak values relative to the signal RMS value [29]. These undesired high peak values can induce harmonic distortions. A means to avoid such harmonic distortions is to control the crest factor (CF) or the Peak to Average Power Ratio (PAPR) [14], respectively measured in voltage ratio or in power ratio. In the LTE, the PAPR is used to measure the transmission signal quality at the PA (Power Amplifier) output [15]. The different definitions of PAPR, depending on the nature of the signals measured, are given in article [29]. In our study, the PAPR calculation is carried out with the oscilloscope. The general definition of a continuous time function power ratio "s(t)" is given by:

$$PAPR\{s(t)\} = \frac{\max |s(t)|^2}{E\{|s(t)|^2\}} \tag{4}$$

where, $E\{|s(t)|^2\}$ defines the expectation operation for a real variable t.

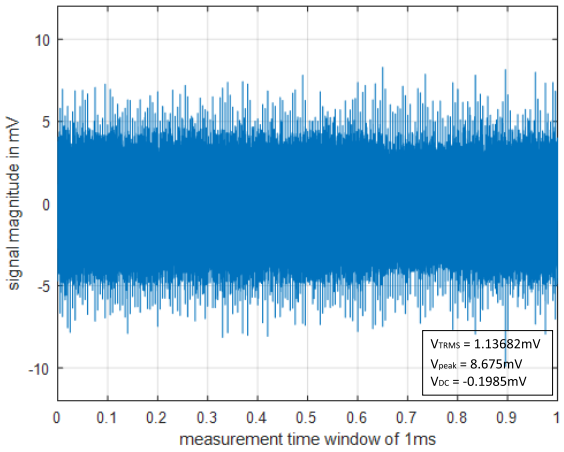

FIGURE 9. Received signal measurement for 5μs repetition time transient interferences.

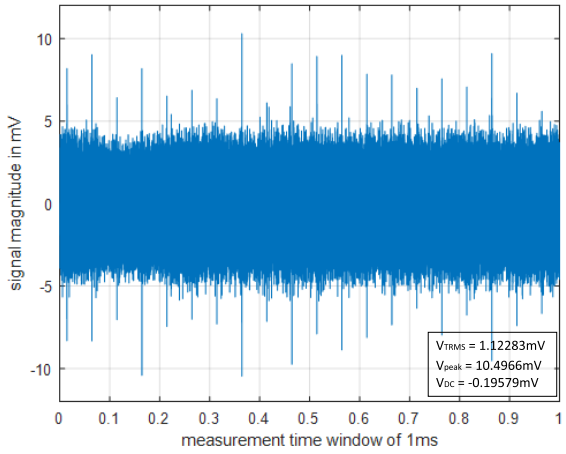

FIGURE 10. Received signal measurement for 50μs repetition time transient interferences.

The LTE signal plus interferences $s_{rx}(nT_s)$ is measured using an oscilloscope over a 1ms window at a sampling frequency of 10Gsps and then recorded to calculate the PAPR. Figure 9 and Figure 10 represent the signals received at the input of the radio-communication tester. The value of $PAPR\{s_{rx}(nT_s)\}$ is calculated from the voltage values $V_{meas}(nT_s)$, V_{DC}.

Under matlab, to calculate the PAPR, first the signal DC component (V_{DC}) is removed from the measured signal $V_{meas}(nT_s)$ to obtain $s_{rx}(nT_s)$. Then the $s_{rx}(nT_s)$ peak value and the $s_{rx}(nT_s)$ RMS value are calculated over a 1ms window. Following the power ratio general definition (4) for a sampled signal, at T_s, with a finite samples number, N, the PAPR is given by:

$$PAPR\{s_{rx}(nT_s)\} = \frac{\max_{n\in[1,NT_s]}\{|s_{rx}(nT_s)|^2\}}{\frac{1}{N}\sum_{n=1}^{N}|s_{rx}(nT_s)|^2} \quad (5)$$

In Equation (5), the signal maximum value over the 1ms oscilloscope window only depends on the transient interference amplitude α, as shown in Figure 10. Indeed, the peak values of the transient interference always exceed the communication signal amplitude. In (5), at the denominator, the average power mainly depends on the LTE communication uplink signal. It is then quasi constant and imposed by the radio-communication tester.

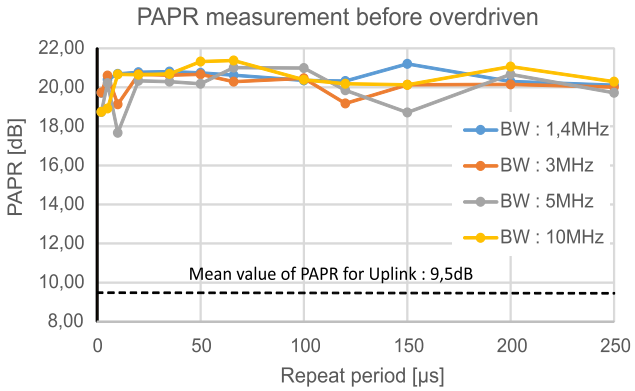

FIGURE 11. PAPR at the communication loss moment as a function of the transient repetition interval time.

Measurements were carried out to calculate the value of the PAPR at the time the communication was cut off. During the experiments, the interference power level was gradually increased, and the oscilloscope windows were collected at each step. The oscilloscope window collected just before the cut off of the LTE communication was then used to calculate the average and peak values involved in Equation (5). The experiment was repeated for different LTE bandwidths and repeat period values of the transient interference. The results giving the PAPR value reached just before the communication cut-off are presented in Figure 11. In order to analyze the PAPR values of Figure 11, the PAPR values of the LTE signal without any transient interference are reported in Table 3, giving values between 9dB and 10dB.

In Figure 11 with the transient interference, the PAPR at the communication cut off reaches values between 18dB and 21dB. Therefore, we notice that the PAPR value at the communication loss moment is almost constant for the different transient interference repetition time values and whatever the LTE communication BW. This value about 20dB can therefore be considered as the limit value that the LTE communication can support. In a conventional context, i.e., without transient interference, this value is never reached. When thermal noise and/or non-transient interference increases, both the EVM and PAPR indicators can increase. However, the EVM can reach the 17.5% limit value without a significant increase in the PAPR, resulting in a communication breakdown due to EVM. Our results show that transient interference, by its nature, has specifically a strong impact on the PAPR value, which means that the 20 dB limit value can be reached without producing a significant increase of the EVM. This is observed for repetition periods greater than 4μs in Figure 7. For repetition periods less than 4μs, the successive interferences are so close that the EVM exceeds the 17.5% limit. However, the communication is not interrupted, whereas the EVM limit is exceeded. These results

TABLE 3. RF Measurements Table of PAPR for a LTE Communication Without Transient Interference

Channel bandwidth	1.4MHz	3MHz	5MHz	10MHz
PAPR values	9.18 dB	9.26dB	9.43dB	9.97dB

show the need to monitor the PAPR in addition to the EVM to detect the risk of LTE communication interruption due to the presence of transient interference. Thus, if a communication interruption occurs with a high PAPR value, then it can be deduced that it is caused by transient interferences. These results therefore constitute a diagnostic aid in the event of communication failures.

VI. CONCLUSION

In this study, the behavior of quality indicators of an LTE communication in the presence of transient interference is presented. The interference model studied is representative of the interference produced by the pantograph catenary sliding contact of high-speed trains. For this transient interference model, we fixed the rise time and the hold time and we studied the influence of other parameters like the repetition interval time and the amplitude. Since EVM is the main quality indicator for digital modulations like LTE, we started our study with this indicator. However, we noticed that the EVM is not sufficient to observe the effect of transient interference on the LTE signal, due to breakdown communications occurring in the presence of transient interference without exceeding the standard EVM limit values. To overcome this lack of representativeness in this railway context, we propose to use another quality indicator, namely the PAPR. Indeed, our investigation results show that communication interruptions are mainly due to a too high dynamic range of the received signal, caused by transient interference occurences. Since the PAPR is used to measure the dynamics of the signal at reception, it is then better suited to analyze the effect of transient electromagnetic interference.

The observation of the PAPR made it possible to establish a scale of limit values between 18 and 21 dB. When these limit values are exceeded, the LTE communication is interrupted, whatever the BW signal and whatever the repetition period of the transient interference. The PAPR appears as a relevant quality indicator to monitor LTE communications carried out in environments rich in electromagnetic transient disturbances. Then, the PAPR should be added to the other quality indicators of LTE communication. Even if LTE (4G) is the current used communication protocol for new railway applications, such as the train remote control, the 5G is probably the future of the railway communication system. Given that 5G also uses OFDM-type modulations, it will remain interesting to measure the PAPR to diagnose the potential impact of transient interference on 5G communications. Hence, the follow-up of the PAPR is still a relevant indicator for 5G. However, the measurement parameters of the PAPR will have to vary depending on the multiple configurations that 5G can take. This could be investigated in further studies. To conclude, this study is a first step in the perspective of bringing a new monitoring system of the LTE communication. The next step would be to validate these results in real conditions, through the number of users and the speed of the train in order to include other factors impacting the communication.

REFERENCES

[1] R. Chen, W.-X. Long, G. Mao, and C. Li, "Development trends of mobile communication systems for railways," *IEEE Commun. Surveys Tuts.*, vol. 20, no. 4, pp. 3131–3141, 4th Quart., 2018.

[2] A. Sniady and J. Soler, "LTE for railways: Impact on performance of ETCS railway signaling," *IEEE Veh. Technol. Mag.*, vol. 9, no. 2, pp. 69–77, Jun. 2014.

[3] R. He, B. Ai, G. Wang, K. Guan, Z. Zhong, A. F. Molisch, C. Briso-Rodriguez, and C. P. Oestges, "High-speed railway communications: From GSM-R to LTE-R," *IEEE Veh. Technol. Mag.*, vol. 11, no. 3, pp. 49–58, Sep. 2016.

[4] R. Lagay and G. M. Adell, "The autonomous train: A game changer for the railways industry," in *Proc. 16th Int. Conf. Intell. Transp. Syst. Telecommun. (ITST)*, Oct. 2018, pp. 1–5.

[5] D. Trentesaux, R. Dahyot, A. Ouedraogo, D. Arenas, S. Lefebvre, W. Schön, and H. Cheritel, "The autonomous train," in *Proc. 13th Annu. Conf. Syst. Syst. Eng. (SoSE)*, Jun. 2018, pp. 514–520.

[6] E. Masson, P. Richard, S. Garcia-Guillen, and G. M. Adell, "TC-rail: Railways remote driving," in *Proc. 12th World Congr. Railway Res.*, Tokyo, Japan, 2019, pp. 1–7.

[7] A. Mariscotti, A. Marrese, and N. Pasquino, "Time and frequency characterization of radiated disturbances in telecommunication bands due to pantograph arcing," in *Proc. IEEE Int. Instrum. Meas. Technol. Conf. Proc.*, Graz, Austria, May 2012, pp. 2178–2182.

[8] J. Wang, G. Wang, D. Zhang, J. Zhang, and Y. Wen, "The influence of pantograph arcing radiation disturbance on LTE-R," in *Proc. Int. Conf. Electromagn. Adv. Appl. (ICEAA)*, Granada, Spain, Sep. 2019, pp. 0583–0586.

[9] S. Rathi, N. Malik, N. I. Chahal, and S. Malik, "Throughput for TDD and FDD 4 G LTE systems," *Int. J. Innov. Technol. Exploring Eng.*, vol. 3, no. 12, pp. 73–77, 2014.

[10] A. Z. Yonis, M. F. L. Abdullah, and M. F. Ghanim, "LTE-FDD and LTE-TDD for cellular communications," in *Proc. Prog.*, 2012, pp. 1467–1471.

[11] M. A. N. Sukar and M. Pal, "SC-FDMA & OFDMA in LTE physical layer," *Int. J. Eng. Trends Technol.*, vol. 12, no. 2, pp. 74–85, 2014.

[12] C. Zhao and R. J. Baxley, "Error vector magnitude analysis for OFDM systems," in *Proc. 14th Asilomar Conf. Signals, Syst. Comput.*, 2006, pp. 1830–1834.

[13] K. Wu, G. Ren, and Q. Wang, "Error vector magnitude analysis of uplink multiuser OFDMA and SC-FDMA systems in the presence of nonlinear distortion," *IEEE Commun. Lett.*, vol. 21, no. 1, pp. 172–175, Jan. 2017.

[14] M. M. Rana, M. S. Islam, and A. Z. Kouzani, "Peak to average power ratio analysis for LTE systems," in *Proc. 2nd Int. Conf. Commun. Softw. Netw.*, Singapore, 2010, pp. 516–520.

[15] Y. Louët and J. Palicot, "A classification of methods for efficient power amplification of signals," *Ann. Telecommun. Annales des télécommunications*, vol. 63, nos. 7–8, pp. 351–368, Aug. 2008.

[16] V. Deniau, N. Ben Slimen, S. Baranowski, H. Ouaddi, J. Rioult, and N. Dubalen, "Characterisation of the EM disturbances affecting the safety of the railway communication systems," in *Proc. IET Colloq. Rel. Electromagn. Syst.*, Paris, France, 2007, pp. 1–5.

[17] N. B. Slimen, V. Deniau, J. Rioult, S. Dudoyer, S. Baranowski, "Statistical characterisation of the EM interference acting on GSM-R antennas fixed above moving trains," *Eur. Phys. J. Appl. Phys.*, vol. 48, no. 2, 2009, Art. no. 21202.

[18] Y. Wen, B. Sun, Q. Wang, and Z. Tan, "Research on the EMI radiation of discharge of pantograph-offline on EMU," in *Proc. Int. Conf. Electromagn. Adv. Appl. (ICEAA)*, Palm Beach, FL, USA, Aug. 2014, pp. 562–565.

[19] S. Chen and F. Sha, "Three types of electromagnetic noise between pantograph and catenary," in *Proc. 3rd IEEE Int. Symp. Microw., Antenna, Propag. EMC Technol. Wireless Commun.*, Beijing, China, Oct. 2009, pp. 40–43.

[20] M. Pous and F. Silva, "APD radiated transient measurements produced by electric sparks employing time-domain captures," in *Proc. Int. Symp. Electromagn. Compat.*, Gothenburg, Sweden, Sep. 2014, pp. 813–817.

[21] H. Fridhi, V. Deniau, J. P. Ghys, M. Heddebaut, J. Rodriguez, and I. Adin, "Analysis of the coupling path between transient EM interferences produced by the catenary-pantograph contact and on-board railway communication antennas," in *Proc. Int. Conf. Electromagn. Adv. Appl. (ICEAA)*, Sep. 2013, pp. 587–590.
[22] G. Boschetti, A. Mariscotti, and V. Deniau, "Assessment of the GSM-R susceptibility to repetitive transient disturbance," *Measurement*, vol. 45, no. 9, pp. 2226–2236, Nov. 2012.
[23] T. Hammi, N. Ben Slimen, V. Deniau, J. Rioult, and S. Dudoyer, "Comparison between GSM-R coverage level and EM noise level in railway environment," in *Proc. 9th Int. Conf. Intell. Transp. Syst. Telecommun., (ITST)*, Lille, France, Oct. 2009, pp. 123–128.
[24] *User Equipment (UE) Radio Transmission and Reception*, document TS 36.101 version 8.9.0 Release 8 2010-04, 3GPP, 2010.
[25] S. Dudoyer, V. Deniau, R. R. Adriano, M. N. B. Slimen, J. J. Rioult, B. Meyniel, and M. M. Berbineau, "Study of the susceptibility of the GSM-R communications face to the electromagnetic interferences of the rail environment," *IEEE Trans. Electromagn. Compat.*, vol. 54, no. 3, pp. 667–676, Jun. 2012.
[26] A. Mariscotti and V. Deniau, "On the characterization of pantograph arc transients on GSM-R antenna," IMEKO, Budapest, Hungary, 2010, pp. 8–10.
[27] *User Equipment (UE) Conformance Specification; Radio Transmission and Reception; Part 1: Conformance Testing*, document TS 36.521-1 version 8.3.1 Release 8 2009-09, 3GPP, 2009.
[28] *LTE RF Measurements With the R&S CMW500 According*, document TS36.521-1, 3GPP, Jenny Chen, May 2014.
[29] J. Palicot and Y. Louët, "Power ratio definitions and analysis in single carrier modulations," in *Proc. 13th Eur. Signal Process. Conf.*, 2005, pp. 1–4.

OLIVIER STIENNE received the engineering degree in electronics engineering from the Cnam Engineering School, Paris, France, in 1999. He is currently pursuing the Ph.D. degree in micro and nanotechnologies, acoustic, and telecommunications with the telecommunications with the Interference and Electromagnetic Compatibility Group, Lille University, Villeneuve d'Ascq, France.

He worked for 10 years in the industry. Then, he joined the E.E.A. Department, Icam, Lille, where he teaches electronics and telecommunications to engineering students. His current research interests include the analysis of the impact of the electromagnetic interference on the performance of wireless communications using orthogonal frequency division multiplexing modulation.

VIRGINIE DENIAU received the M.S. and Ph.D. degrees in electronics from the Lille University, Lille, France, in 2000 and 2003, respectively. Since 2003, she has been a Researcher in electromagnetic compatibility (EMC) with the French Institute of Science and Technology for Transport, Development, and Networks, Villeneuve d'Ascq, France. She conducts works on EMC for land transport. She is currently involved in the hardening of land transport systems regarding cyber-attacks, such as electromagnetic attacks. She has participated in numerous National and European projects. Her research interests include EMC test facilities and methodologies, the characterization and modeling of electromagnetic transport environments, and the immunity test methodologies for embedded systems. She was a Scientific Coordinator of the European Union's Research and Innovation Funding Program and 2007–2013 (FP7) project SECRET for Security of Railways against Electromagnetic Attacks. She is also the Vice-Chair of the URSI Committee E (Electromagnetic Interference).

ERIC PIERRE SIMON received the M.S. degree in electronics engineering from the Superior School of Electronics, Lyon, France, in 1999, and the Ph.D. degree in signal processing and communications from the National Polytechnic Institute of Grenoble (INPG), Grenoble, France, in 2004. In 2005, he was a Teaching Assistant with INPG. In 2006, he joined one of France Telecom R&D Laboratories as a Postdoctoral Fellow. He is currently an Associate Professor with the Institute of Electronics, Microelectronics and Nanotechnology, Telecommunications, Interference and Electromagnetic Compatibility Group, Lille University, Villeneuve d'Ascq, France. His current research interests include mobile communications and carrier and symbol synchronization.